RSC Advances

ROYAL SOCIETY OF CHEMISTRY

www.rsc.org/advances

Journal Name

ARTICLE

Photoresponsive structure transformation and emission enhancement based on a tapered azobenzene gelator

Received 00th January 20xx,
Accepted 00th January 20xx

DOI: 10.1039/x0xx00000x

www.rsc.org/

Lili Shi[a], Xia Ran[a] *, Yajie Li[a], Qiuyue Li[a], Weihong Qiu[b] and Lijun Guo [a]*

A new low molecular mass organic gelator bearing 1,3,4-oxadiazole and azobenzene groups, namely N-(3,4,5-tributoxyphenyl)-N'-4-[(4-hydroxyphenyl)azophenyl] 1,3,4-oxadiazole (AOB-t4), was designed and synthesized in this work. The organogelator shows a great ability to gel moderate polar solvents and form stable organogels with the critical gelation concentration as low as 2.0 mg/mL, which thus can be considered as a supergelator. The morphology of xerogels demonstrates a strong dependence on the nature of gelling solvents. Due to the photo-induced isomerization of azobenzene unit, the transformations from fiberous to porous structure in AOB-t4 dichloromethane gel, and from fiber to nanoparticle in ethanol solution have been successfully achieved with UV 365 nm irradiation, respectively. Meanwhile, an enhanced fluorescence via *J*-aggregate molecular arrangement can be observed with the *trans*-to-*cis* photoisomerization in both dichloromethane gel and ethanol solution of AOB-t4, and the emission quantum yield can be increased from 10.7×10^{-5} to 18×10^{-2} in ethanol, corresponding to 1682 times enhancement. The obtained results would be of significance in developing novel photo-controllable luminescence molecular device and broadening the application fields of azobenzene derivatives.

Introduction

In the past decades, supramolecular gels based on low molecular mass organogelators, which are capable of forming gels with organic liquids at relatively low concentration through non-covalent interactions, have attracted broad attention.[1] Supramolecular self-assembly is the spontaneous process of molecular aggregation and provides us a bottom-up approach to obtain structural regularity of various morphologies such as fibers, particles, tubes and helical ribbons.[2] However, a complete mechanism for the self-assembled supramolecular structure is still beyond our understanding. Recently, there has been a rapidly growing interest in tuning morphology by changing the molecular structures,[3] the composition of binary gels,[4] solvents,[5] as well as using ultrasound,[6] light[7] and so on. For example, Rogers and co-workers reported the nanostructure, microstructure and supramolecular structures of hydroxyl stearic acid molecule gels are all influenced by the chemical nature of solvents and correlated to the hydrogen-bonding Hansen solubility parameter.[5a] Yi and co-workers demonstrated that the morphology and luminescence of a cholesterol based terpyridyl-Pt metallogel can be reversibly adjusted by sonication and heating.[6a] Compared to other induction factors, light is considered as an ideal means to control the morphology of organogels due to the noncontact feature and site-specific fashion.[7] Feringa and co-workers presented that the incorporation of the light-switchable functionality allows the photochemical control over vesicle formation in water and the light-controlled self-assembly fibers in aromatic solvents.[7a]

Photoresponsive azobenzene moieties have been widely used in supramolecular chemistry, catalysis, and materials science,[8-10] and a large number of gelators comprising azobenzene units have been reported.[11] For instance, Hughes et al. observed the photocontrolled gel-sol phase transition based on a reactive azobenzene gelator in a range of hydrophobic solvents.[11a] Huang and co-workers reported a dual-responsiveness of the molecular recognition motif between a new thermoresponsiveness of pillar[7] arene and photoresponsiveness of azobenzene.[11b] Although much effort has been devoted to achieve a good gelation with light responsive property, little attention is paid to the structural characteristics and fluorescence emissions of *cis*-azobenzene aggregates formed from the destroying of gel state, which is generally supposed to consist of small pieces of fibers and non-fluorescence components in solution with imperceptible quantum yields.

In general, it is a known fact that azobenzene molecules do not fluoresce with imperceptible quantum yields due to the low *trans–cis* isomerization.[11d, 11m] The emitting azobenzenes have been expected to be powerful candidates as fluorescent materials and devices, fluorescent probes, and molecular detectors, because of the variety of archived methods for

[a]*Department of Physics, School of Physics and Electronics, Henan University, Kaifeng 475004, People's Republic of China. E-mail: ranxia@henu.edu.cn, juneguo@henu.edu.cn*
[b]*Department of Physics, Oregon State University, Corvallis OR 97331, USA.*
† Xia Ran contributed with Lili Shi, and they are both the first author.
Electronic Supplementary Information (ESI) available: See
DOI: 10.1039/x0xx00000x

synthesizing azobenzenes and tuning their properties. Recently, a few reports have been presented on fluorescence emission which is taking advantage of aggregation-induced emission (AIE).[11j, 11n, 12] Luminophores possessing the property of AIE discovered by Tang and co-workers, have attracted attention as promising materials for electroluminescent devices and optical sensing.[13] For instance, Han and co-workers observed the photoinduced formation of blue fluorescent for simple azobenzene derivatives with different alkyl chain lengths, which is attributed to the light driven self-assembly of cis-azobenzenes.[11j] Zhu and co-workers reported that the azobenzene polystyrene can self-assemble to nanoscale aggregation under the UV-irradiation and show strong fluorescence emission from azobenzene chromophore.[12] To date, a complete mechanism for the fluorescent emission of azobenzene derivatives is still beyond our understanding. It is essential to further explore fluorescent azobenzene-containing derivatives by carrying out deep investigation to understand the fluorescence behaviour.

Here, we report the synthesis of an azobenzene-contained gel system, N-(3,4,5-tributoxyphenyl)-N'-4-[(4-hydroxyphenyl) azophenyl] 1,3,4-oxadiazole (AOB-t4) (Scheme 1), and investigate the gelation property and the phase transition of AOB-t4 under light stimuli. A photoinduced and solvent mediated morphological transformation and a significant fluorescence enhancement are observed in AOB-t4 self-assembly structure, and a possible mechanism is also proposed in this work.

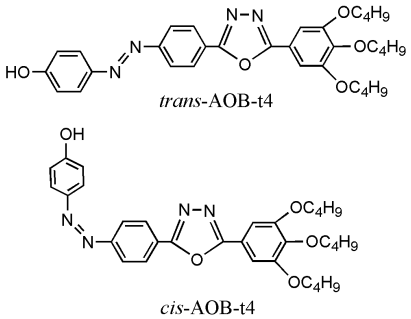

Scheme 1 Molecular structure of AOB-t4.

Experimental

Synthesis

The compound, N-(3,4,5-tributoxyphenyl)-N'-4-[(4-hydroxyphenyl) azophenyl] 1,3,4-oxadiazole (AOB-t4), was synthesized through the route similar to that shown in reference.[14] The hydrazine derivatives BNB-t4 were prepared by the protocol described in our previous work.[14] Briefly, the purified BNB-t4 was dissolved in phosphorous oxychloride ($POCl_3$) and refluxed for about 40 h. The excess $POCl_3$ was removed through distillation and the residue was slowly added into ice-water. After the removal of solvent under reduced pressure, the final product AOB-t4 was purified by recrystallization from ethanol for further NMR, FT-IR spectroscopy and elemental analysis.

N-(3,4,5-tributoxyphenyl)-N'-4-[(4-hydroxyphenyl)azophenyl] 1,3,4-oxadiazole (AOB-t4)

^{1}H NMR (400MHz, DMSO-d_6), (ppm, from tetramethylsilane): 8.37(d, 2H, J=8.4), 8.08(d, 2H, J=8.8), 7.98(d, 2H, J=8.8), 7.41(d, 2H, J=8.8), 7.35(s, 2H), 4.12-3.94(m, 6H), 1.80-1.62(m, 6H), 1.56-1.45(m, 6H), 0.99-0.93(m, 9H).

FT-IR (KBr, pellet, cm^{-1}): 3429, 2958, 2932, 2874, 1595, 1554, 1492, 1466, 1438, 1388, 1326, 1294, 1232, 1123, 1029, 976, 921, 854, 748, 727.

Elemental analysis: calculated for $C_{32}H_{38}N_4O_5$ (%): C, 68.8; H, 6.86; N, 10.03. Found: C, 68.57; H, 6.95; N, 9.82.

Melting point of AOB-t4 powder: 185 ^{o}C.

Characterization

All the solvents for spectral measurements were of spectroscopic grade and used as received. ^{1}H NMR spectra were recorded with an Avance-400 400 MHz spectrometer, using tetramethylsilane (TMS) as an internal standard. Field emission scanning electron microscopy (FE-SEM) images were taken with a JSM-6700F apparatus. Samples for FE-SEM measurement were prepared by wiping a small amount of gel and solution onto a silicon plate and followed by drying in a vacuum for 12 h at 15^{o}C. FT-IR spectra were recorded with a Perkin-Elmer spectrometer (Spectrum One B). The xerogels were obtained by freezing and pumping the organogel of AOB-t4 for 12 h, and then pressed into a tablet with KBr for FT-IR measurements. A 500 W super pressure Hg lamp with an appropriate-filter (320 < λ < 390 nm for UV light) were employed in the photoirradiation experiments, and the UV light intensity was set to be ca. 30 mW cm^{-2} at the surface of quartz cuvette. The UV-vis absorption spectra were obtained on a PerkinElmer Lambda 35 spectrometer. Photoluminescence spectra were collected by a PerkinElmer LS55 spectrophotometer. The room-temperature luminescence quantum yields in solutions were determined relative to quinine sulfate in sulfuric acid aqueous solution (0.546) and calculated according to the equation: $\Phi_{unk}=\Phi_{std}(I_{unk}/A_{unk})(A_{std}/I_{std})(n_{unk}/n_{std})$,[15] in which Φ_{unk} is the quantum yield of sample; Φ_{std} is the emission quantum yield of standard; I_{unk} and I_{std} are the integrated emission intensities of the sample and standard, respectively; A_{unk} and A_{std} are the absorbance of sample and standard at the excitation wavelength, respectively; n_{unk} and n_{std} are the indexes of refraction of the sample and standard solutions (pure solvents were assumed), respectively.[16]

Gelation test: The weighted gelator was mixed in a cap sealed test tube [3.5 cm (height) × 0.5 cm (radius)] with an appropriate amount of solvent, and the mixture was heated until the solid dissolved. The sample vial was cooled to 4 ^{o}C and then turned upside down. When a clear or slightly opaque gel formed, the solvent therein was immobilized at this stage. The gel melting temperature (T_m) was determined by the "falling drop" method.[17] An inverted gel was immersed in a water bath initially at or below room temperature, and then was heated slowly up to the point at which the gel fell due to the force of gravity, i.e. the T_m.

Results and discussion

Molecular Design and Gelation Properties

The noncovalent interactions, such as hydrogen bonding, π-π stacking and Van der Waals interaction, play a mutual balance to modulate the packing arrangement of molecules and eventually construct a particular superstructure and functional surface. To employ the aforementioned interactions and drive the self-assembly gelation, we designed and synthesized a tapered oxadiazole derivative AOB-t4, containing hydroxyl, azobenzene, 1,3,4-oxadiazole moieties, and three alkyl chains (Scheme 1). The numerous interactions in AOB-t4 should offer, at least to some extent, the possibility in controlling the aggregation morphology of organogel. From the investigation of gelation properties for AOB-t4 in several different solvents, the corresponding minimum gel concentration is summarized in Table 1. The results indicate the AOB-t4 can form stable gel in moderate polar solvents such as dichloromethane, chloroform and acetone, while is dissolved in strong polar solvents and insoluble in non-polar solvents. Specifically, AOB-t4 demonstrates a stronger gelation ability in dichloromethane than in other solvents, with a critical gel concentration (CGC) as low as 1.3 mg/mL (0.09 wt %), which thus can be considered as a supergelator. The melting temperatures (T_m) of AOB-t4 gel in dichloromethane dichloromethane, chloroform and acetone as a function of concentration are shown in Figure 1, reflecting the thermally gel-sol phase transition property in different solvents of AOB-t4. It can be seen that the T_m rises from 20 °C to 63 °C as the concentration of AOB-t4 increasing from 2 mg/mL to 14 mg/mL, and the T_m at the plateau region is higher than the boiling point of dichloromethane (39.8 °C). In contrast, the value of the T_m in the "plateau region" decreases from 75 °C in chloroform to 48 °C in acetone. Figure 2a shows the SEM image of xerogel AOB-t4 from dichloromethane, it can be observed that a developed and tightly stacked network is constructed from dense and entangled fibers with the width of 50-60 nm. For the xerogel of AOB-t4 from acetone (Figure 2b), the morphology shows a cloudlike and 3D cross-linking network structure. Interestingly, SEM images (Figure 2c and Figure 2d) of AOB-t4 xerogel from chloroform reveal a multilayer feature, in which the upper layer exhibits irregular honeycomb matrix with the pore size of 1.4-6.5 μm and wall thickness of about 280 nm, and the lower layer consists of flexible fibers with the width of 50-60 nm. These observations indicate that the morphology of the xerogels strongly depends on the nature of the gelling solvents and the self-assembly of AOB-t4 is driven by strong intermolecular interactions.

Table 1 Gelation properties[a, b] of AOB-t4

Solvent	State	CGC	Solvent	State	CGC
Cyclohexane	I	-	chloroform	G	4.7
benzene	P	-	acetone	G	7
Tetrahydrofuran	P	-	ethanol	S	-
DMF	G	1.3	DMSO	S	-

[a]I: insoluble; G: stable gel formed at room temperature; P: precipitate; S: soluble; CGC: critical gelation concentration (mg/mL), the minimum concentration necessary for gelation of solvents. [b]DMSO: dimethyl sulfoxide; DMF: dimethylformamide.

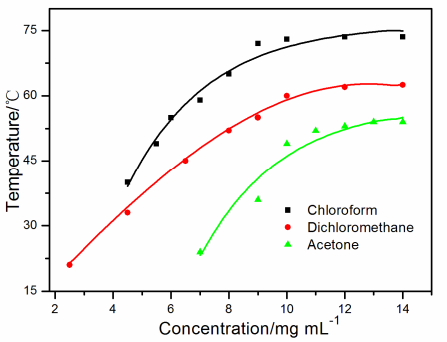

Figure 1 Concentration-dependent melting temperature (T_m) of AOB-t4 gels in dichloromethane, chloroform and acetone.

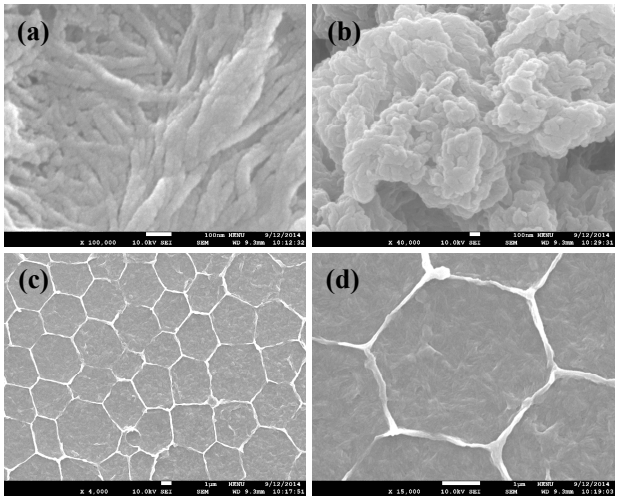

Figure 2 SEM images of AOB-t4 xerogels from (a) dichloromethane, (b) acetone and (c, d) chloroform.

Photoisomerization studies

Photoisomerization is expected to induce the changes of self-assembled structure and fluorescence properties of AOB-t4. Upon irradiation by UV light, we observed that the *trans*-AOB-t4 organogel in dichloromethane collapsed and the subsequent sol of *cis*-AOB-t4 (Figure 3) formed. This phase transition can be further confirmed by monitoring the UV-visible spectroscopy evolution of AOB-t4 gel in dichloromethane (2 mg/mL). Figure 4a shows the typical absorption spectra with different time period under 365 nm irradiation. It can be observed that the maximum π-π* absorption band at 361 nm of *trans*-azobenzene moiety decreases with the irradiation time, while that of *cis*-azobenzene at 278 nm (n-π* absorption band) increases concomitantly, indicating the photoinduced *trans*-to-*cis* isomerization takes place and eventually brings about the gel-sol transition. The conversion efficiency of *cis*- azobenzene can

reach ca. 85% at the photo-stationary state within 280 min, estimated on the basis of UV-vis absorption spectra.[18]

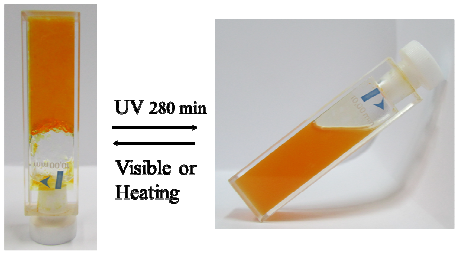

Figure 3 Photographs of the dichloromethane gel of AOB-t4 (2.0 mg/mL) before (left) and after (right) UV irradiation (365 nm).

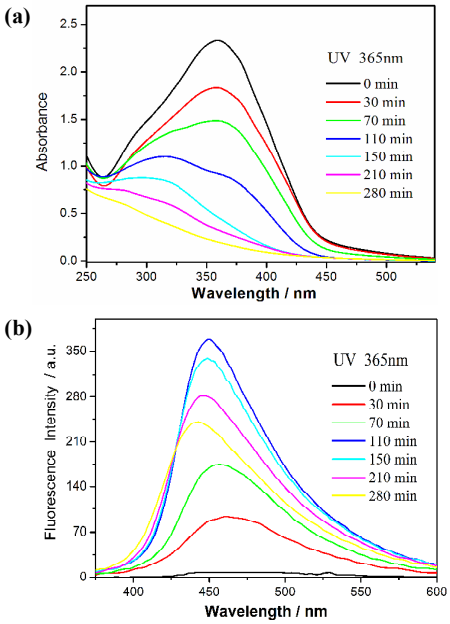

Figure 4 (a) UV-vis spectra and (b) fluorescence spectra of AOB-t4 in dichloromethane (2.0 mg/mL) under irradiation at 365 nm for different time period at room temperature.

Figure 5a and Figure 5b show the SEM images of AOB-t4 organogel in dichloromethane after exposure to 365 nm light for 110 min and 280 min, respectively. Compared with the situation shown in Figure 2a, it can be observed that the fiber edge become blurred, and some fibers merge with one another after 110 min UV irradiation. With further UV exposure and fiber merging, a porous structure in a large area with a non-uniform pore size is observed in 280 min. The pores exhibit different shapes, round, oval, square and rectangle, and different pore size ranging from 25 nm to 750 nm. In a word, the SEM observations of AOB-t4 morphology in dichloromethane demonstrate a photoinduced fiber-to-porous structure morphology evolution in coordination with solvent.

On the other hand, the photoisomerization also shows the effect on modulating the photophysical properties of AOB-t4 dichloromethane gel. Upon 320 nm excitation (figure 4b), the AOB-t4 gel in dichloromethane shows a very weak fluorescence with the emission maximum at 475 nm, and the fluorescence quantum yield is of 11.7×10^{-5}. However, an increasing fluorescence can be activated with continuous exposure to UV light and the emission maximum is blue-shifted to 461 nm in 30 min. The continuous emission intensity increasing within 110 min can be observed and attributed to the emission of *cis*-AOB-t4 as shown in Figure 4b. With the irradiation time from 30 to 280 min, the fluorescence spectra clearly demonstrate an evolution feature, from an increasing and blue-shifting Gaussian emission to a decreasing by appearance and blue-shifting non-Gaussian fluorescence spectrum. The apparent weakening emission after 280 min UV irradiation is ascribed to the decreasing absorption section at

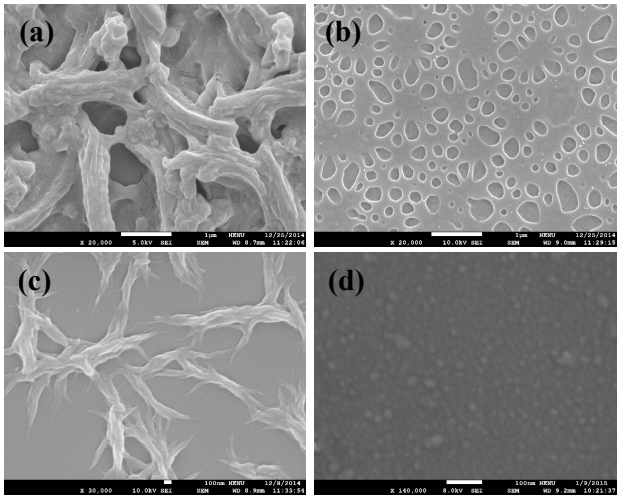

Figure 5 SEM images of AOB-t4 (a) in dichloromethane (2.0 mg/mL) after exposure to UV light for 110 min and (b) 280 min, (c) in ethanol (2.0 mg/mL) before exposure to UV light and (d) under irradiation at 365nm for 260 min.

excitation wavelength (Figure 4a). As a matter of fact, the quantum yield is improved to 2.1×10^{-2}, enhanced by 180 times than that of the initial solution. The non-Gaussian spectrum actually arises from different emission contributions of monodispersed and aggregated *cis*-AOB-t4. In other words, the significant blue-shifted emission and evolved spectral structure is originated from both the photoisomerization and the formation of *cis*-AOB-t4 aggregates.

To explore the effect of solvent polarity on the self-assembled structure, we investigated the aggregation pattern of AOB-t4 in ethanol. When a concentrated (2.0 mg/mL) solution of AOB-t4 in ethanol were continuously exposed to UV light, the UV-vis spectroscopy (Figure 6a) shows the typical change of photoinduced *trans-cis* isomerization, which is similar to that of AOB-t4 in dichloromethane (Figure 4a). However, a different morphology transformation can be observed much clearly for AOB-t4 in ethanol as shown in Figure 5c and Figure 5d. Without exposure to UV light, the structure of aggregates is characterized by short and flexible root-like fibers with the width of 100-150 nm and the length of

several micrometers. After exposed to UV light for 260 min, SEM image suggests the formation of poly-dispersed spherical structure, with an average diameter of about 25 nm (Figure 5d). Meanwhile, the spherical nanoparticles can partially aggregate to generate agglomerates, indicating that larger spheres are formed by the fusion of smaller ones. In other words, the AOB-t4 in ethanol demonstrates a fiber-to-nanoparticle morphology evolution under UV irradiation. So far, the structure transformations, from fiber to porous structure in dichloromethane and from fiber to nanoparticle in ethanol, with the cooperation of photo-inducement and solvent effect have been successfully observed.

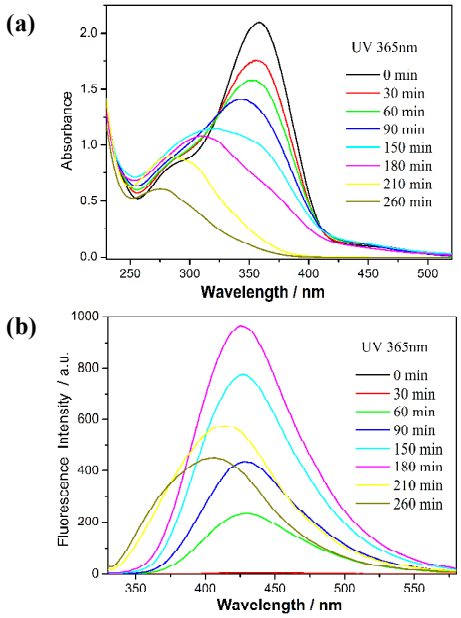

Figure 6 (a) UV-vis spectra and (b) fluorescence spectra of AOB-t4 in ethanol (2.0 mg/mL) under irradiation at 365 nm for different time period at room temperature.

According to the aforementioned results with and without UV irradiation, the solvent polarity demonstrates a distinct effect on the aggregate morphology of AOB-t4. Therefore, it is expected to observe a significant influence of solvent on photophysical properties. When a concentrated (2.0 mg/mL) solution of AOB-t4 in ethanol was continuously exposed to UV light, a remarkable increasing fluorescence confirms the solvent polarity modulating effect on AOB-t4 emission (Figure 6b). Surprisingly, the quantum yield of AOB-t4 in ethanol (2.0 mg/mL) after UV irradiation to balance state is sharply improved to 18×10^{-2}, and enhanced by 1682 times compared to that of the initial nonirradiated solution (the quantum yield is 10.7×10^{-5}), which far exceeds that of AOB-t4 in dichloromethane. As a consequence, the image displays a bright blue violet colour, presenting a striking contrast to the non-fluorescent case without UV light irradiation (Figure 7). Meanwhile, the response rate to UV light of AOB-t4 in ethanol is slightly faster than that of AOB-t4 in dichloromethane.

To obtain deep insight into the self-assembled structure dependence of fluorescence enhancement, the photophysical properties of azobenzene solution with different concentrations ranging from 1×10^{-5} to 1×10^{-3} M were investigated. As shown in Figure S1, without UV irradiation, the fluorescence quantum yield initially decreases with increasing concentration. The most concentrated solution (1×10^{-3} M) is almost nonfluorescent before UV light irradiation, due to the concentration quenching effect. In contrast to the case with UV light irradiation (Figure S2), the UV-vis spectra of a AOB-t4 dilute (1×10^{-5} M) solution in ethanol shows a typical evolution process that, the π-π* absorption of trans-azobenzene moiety at 365 nm decreases with the irradiation time, indicating that photoinduced *trans*-to-*cis* isomerization takes place. When the dilute solution of AOB-t4 was excited at 320 nm, a very weak fluorescence with the maximum at 440 nm was observed, with a fluorescence quantum yield of 9×10^{-4}. However, an increasing fluorescence was activated after the solution was continuously exposed to UV light. The fluorescence spectrum exhibits a broad and blue-shifted band, and the quantum yield is improved to 10×10^{-2} after UV light irradiation, which can be attributed to the emission of monomeric *cis*-AOB-t4. Interesting, the quantum yield after UV irradiation to balance state is sharply improved to 18×10^{-2} for concentrated solution (Figure 6) which is much higher than that of a dilute (1×10^{-5} M) *cis*-AOB-t4 solution. The further enhancement indicates the correlation between emission and molecular aggregation structure, which is so called aggregation-induced emission enhancement.

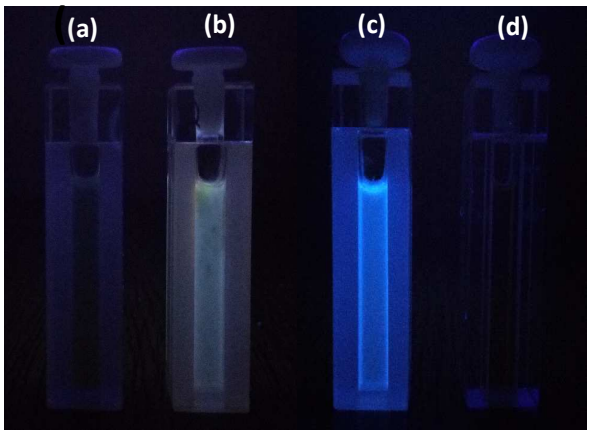

Figure 7 Photographs of AOB-t4 organgel in dichloromethane (2.0 mg/mL) (a)before exposure to UV light and (b) after irradiation at 365 for 280 min; AOB-t4 solution in ethanol (2.0 mg/mL) (c) before exposure to UV light and (d) after irradiation at 365 nm for 260 min.

Besides solvent mediation, the molecular arrangement, interactions and alkyl chain conformations could also contribute the emission enhancement and structural characteristics of self-assembled aggregate from *trans*-to-*cis* AOB-t4, which can be discriminated from the spectroscopy measurements. FT-IR spectroscopy (Figure 8a) of *trans*-AOB-t4

powder from ethanol solution before the irradiation of UV-light shows that the hydrogen-bonded O-H stretching is at 3434 cm^{-1}, while the peak is slightly shifted to the lower wavenumber of 3395 cm^{-1} after the irradiation of 365 nm UV-light for 260 min (Figure 8b). This shift suggests that the hydrogen bond in the *cis*-AOB-t4 aggregated state is stronger than that in the *trans*-AOB-t4 aggregated state. [19] On the other hand, the $v_s(CH_2)$ and $v_{as}(CH_2)$ are at 2871 and 2929 cm^{-1}, respectively, for the *trans*-AOB-t4 powder (Figure 8a), implying that the alkyl chains are tightly packed to form quasi-crystalline domains. Correspondingly, the $v_s(CH_2)$ and $v_{as}(CH_2)$ in the *cis*-AOB-t4 powder (Figure 8b) are located at 2853 and 2921 cm^{-1}, respectively, indicating increased population of the *trans* conformation of alkyl chains in the *cis*-AOB-t4 powder.[20]

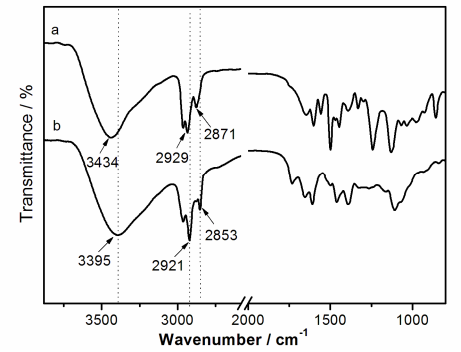

Figure 8 FT-IR spectra of AOB-t4 power from ethanol (a) before and (b) after the irradiation of 365 nm UV-light for 260 min.

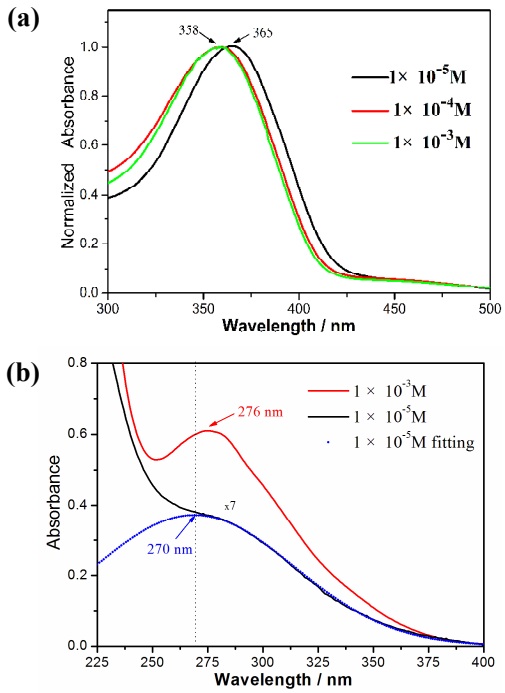

Figure 9 (a) Normalized UV-vis absorption spectra of AOB-t4 in ethanol at different concentration, (b) original and fitting UV-vis absorption spectra of 1×10^{-5} M (black and blue) and 1×10^{-3} M (red) in ethanol after 365 nm irradiation for 260 min, respectively.

Furthermore, the absorption spectra of *trans*-AOB-t4 manifest a slight but detectable dependence on concentration in ethanol as shown in Figure 9a. With the concentration increasing from 1×10^{-5} M to 1×10^{-3} M, the absorption maximum is blue-shifted from 365 nm to 358 nm, specifying the formation of H-aggregates.[21] In other words, the observed quantum yield decreasing with concentration without UV irradiation could be attributed to concentration-quenching or the formation of H-aggregates. In contrast, the n-π* absorption maximum of *cis*-azobenzene group of AOB-t4 is at 270 nm in a dilute (1×10^{-5} M) solution and red-shifts to 276 nm in the most concentrated solution (1×10^{-3} M). This spectroscopic difference for *cis*-AOB-t4 demonstrates that the azobenzene units are arranged into *J*-type aggregates through π-π interactions (Figure 9b).[21] Therefore, the fact that the H-aggregates might be the reason for a low quantum yield observed for the most concentrated solution of *trans*-AOB-t4 in ethanol. Accordingly, the high fluorescence quantum yield for the most concentrated solution of *cis*-AOB-t4 could be attributed to the formation of *J*-aggregates, which leads to the structural variety from fiber to nanoparticle.

Conclusions

We have successfully prepared a gelator (AOB-t4) containing hydroxyl, azobenzene and 1,3,4-oxadiazole moieties, and three alkyl chains. The AOB-t4 shows strong gelation ability in moderate polar solvents such as dichloromethane, chlorofrom and acetone. The minimum gel concentration of AOB-t4 in dichloromethane is as low as 2.0 mg/mL, which can be considered as a supergelator. The morphology of AOB-t4 xerogels strongly depends on the nature of gelling solvents. The photoinduced fiber-to-porous in dichloromethane and fiber to nanoparticle in ethanol structure transformation have been achieved by UV irradiation on gels and solution, respectively. The *trans*-to-*cis* photoisomerization of AOB-t4 is followed by a significant fluorescence enhancement via *J*-aggregate molecular arrangement accompanying with the spontaneous formation of spherical aggregates. The quantum yield of AOB-t4 in ethanol solution after UV irradiation to balance state is sharply improved to 18×10^{-2}, enhanced by 1682 times compared to that of the initial nonirradiated solution.

Acknowledgements

The authors are grateful to the National Science Foundation Committee of China (project No. 21173068) and the Program for Innovative Research Team in University of Henan Province (No. 13IRTSTHN017) for their financial support of this work.

Notes and references

1 (a) J. M. Lehn, Supramolecular Chemistry: Concepts and Perspectives. VCH Weinheim 1995; (b) T. F. A. De Greef, M. M. J. Smulders, M. Wolffs, A. P. H. J. Schenning, R. P.

Sijbesma and E. W. Meijer, *Chem. Rev.,* 2009, **109**, 5687-5754; (c) R. G. Weiss, *J. Am. Chem. Soc.*, 2014, **136**, 7519.
2 (a) S. S. Babu, V. K. Praveen, and A. Ajayaghosh, *Chem. Rev.*, 2014, **114**, 1973; (b) Y. Liu, Z. Wang, X. Zhang, *Chem. Soc. Rev.,* 2012, **41,** 5922.
3 S. N. Qu, H. T. Wang, Z. X. Yu, B. L. Bai and M. Li, *New J. Chem.*, 2008, **32**, 2023.
4 K. Jang, J. M. Kinyanjui, D. W. Hatchett and D.-C. Lee, *Chem. Mater.*, 2009, **21**, 2070.
5 (a)S. Wu, J. Gao, T. J. Emge and M. A. Rogers, *Soft Matter,* 2013, **9**, 5942; (b)P. Zhu, X. Yan, Y. Su, Y. Yang, and J. Li, *Chem. Eur. J.*, 2010, **16**, 3176.
6 (a) K. Liu, L. Meng, S. Mo, M. Zhang, Y. Mao, X. Cao, C. Huang and T. Yi, *J. Mater. Chem. C*, 2013, **1**, 1753; (b) R.-Y. Wang, X.-Y. Liu and J.-L. Li, *Cryst. Growth Des.*, 2009, **9**, 3287.
7 (a) J. T. van Herpt, J. Areephong, M. C. A. Stuart, W. R. Browne, and B. L. Feringa, *Chem. Eur. J.,* 2014, **20**, 1737; (b) X. Ran, H. Wang, P. Zhang, B. Bai, C. Zhao, Z. Yu. and M. Li, *Soft Matter*, 2011, **7**, 8561; (c) H. Jiang, S. Kelch and A. Lendlein, *Adv. Mater.*, 2006, **18**, 1471.
8 (a) M. Russew and S. Hecht, *Adv. Mater.*, 2010, **22**, 3348; (b) H. amaguchi, Y. Kobayashi, R. Kobayashi, Y. Takashima, A. Hashidzume and A. Harada, *Nat. Commun.*, 2012, **3**, 603.
9 (a)A. Natansohn and P. Rochon, *Chem. Rev.*, 2002, **102**, 4139; (b) J. A. Delaire and K. Nakatani, *Chem. Rev.*, 2000, **100**, 1817; (c) C. J. Barrett, J. Mamiya, K. G. Yagerc and T. Ikeda, *Soft Matter*, 2007, **3**, 1249; (d) Y. Zhao and J. He, *Soft Matter,* 2009, **5**, 2686. (e) Z. Li, W. Wu, C. Ye, J. Qin and Z. Li, *Polym. Chem.*, 2010, **1**, 78.
10 (a) D. Hore, A. Natansohn and P. Rochon, *J. Phys. Chem. B*, 2003, **107**, 2197; (b) E. Ishow, B. Lebon, Y. N. He, X. G. Wang, L. Bouteiller, L. Galmiche and K. Nakatani, *Chem. Mater.,* 2006, **18**, 1261; (c) B. L. Lachut, S. A. Maier, H. A. Atwater, M. J. A. de Dood, A. Polman, R. Hagen and S. Kostromine, *Adv. Mater.,* 2004, **16**, 1746; (d) Q. Zeng, Z. A. Li, Z. Li, C. Ye, J. G. Qin and B. Z. Tang, *Macromolecules*, 2007, **40,** 5634;
11 (a) R. Yang, S. Peng and T. C. Hughes, *Soft Matter*, 2014, **10**, 2188; (b) X. Chi, X. Ji, D. Xia, and F. Huang, *J. Am. Chem. Soc.,* 2015, **137**, 1440; (c) W. Xiao, X. Zeng, H. Lin, K. Han, H. Jia, X. Zhang, *Chem. Commun.,* 2015, **51**, 1475; (d) A. Cembran, F. Bernardi, M. Garavelli, L. Gagliardi, and G. Orlandi, *J. Am. Chem. Soc.*, 2004, **126**, 3234; (e) J. Yoshino, A. Furuta, T. Kambe, H. Itoi, N. Kano, T. Kawashima, Y. Ito, and M. Asashima, *Chem. Eur. J.*, 2010, **16**, 5026; (f) J. Yoshino, N. Kano, T. Kawashima, *Dalton Trans.,* 2013, **42**, 15826; (g) K. Tsuda, G. C. Dol, T. Gensch, J. Hofkens, L. Latterini, J. W. Weener, E. W. Meijer, and F. C. De Schryver, *J. Am. Chem. Soc.,* 2000, **122**, 3445; (h) Y. Li, N. Zhou, W. Zhang, F. Zhang, J. Zhu, Z. Zhang, Z. Cheng, Y. Tu, X. Zhu, *J. Polym. Sci., Part A: Polym. Chem.*, 2011, **49**, 4911; (i) F. Ma, N. Zhou, J. Zhu, W. Zhang, L. Fan, X. Zhu, *Eur. Polym. J.*, 2009, **45**, 2131; (j) M. Han and M. Hara, *J. Am. Chem. Soc.*, 2005, **127**, 10951; (k) M. Han, Y. Hirayama, and M. Hara, *Chem. Mater.*, 2006, **18**, 2784; (l) M. Han, D. Ishikawa, E. Muto, M. Hara, *Journal of Luminescence*, 2009, **129**, 1163. (m) H. Rau, *Angew. Chem., Int. Ed. Engl.*, 1973, **12**, 224. (n) M. Han, Y. Hirayama and M. Hara, *Chem. Mater.,* 2006, **18**, 2784.
12 (a) J. Xu, W. Zhang, N. C. Zhou, J. Zhu, Z. P. Cheng, Y. Xu and X. L. Zhu, *J. Polym. Sci., Part A: Polym. Chem.*, 2008, **46**, 5652; (b) Y. Xiang, X. Q. Xue, J. Zhu, Z. B. Zhang, W. Zhang, N. C. Zhou and X. L. Zhu, *Polym. Chem.*, 2010, **1**, 1453.
13 (a) Y. Hong, J. W. Y. Lamab and B. Z. Tang, *Chem. Soc. Rev.*, 2011, **40**, 5361; (b) J. Luo, Z. Xie, J. W. Y. Lam, L. Cheng, H. Chen, C. Qin, H. S. Kwok, X. Zhan, Y. Liu, D. Zhu and B. Z. Tang, *Chem. Commun.*, 2001, 1740; (c) Y. Hong, J. W. Y. Lam and B. Z. Tang, *Chem. Commun.*, 2009, 4332.
14 X. Ran, H. Wang, J. Lou, L. Shi, B. Liu, M. Li and L. Guo, *Soft Mater.,* 2014, **12**, 396.
15 (a) C. W. Tang and S. A. VanSlyke, *Appl. Phys. Lett.*, 1987, **51**, 913; (b) J. H. Burroughes, D. D. C. Bradley, A. R. Brown, R. N. Marks, R. H. Friend, P. L. Burn and A. B. Holmes, *Nature*, 1990, **347**, 539.
16 K. Q. Ye, J. Wang, H. Sun, Y. Liu, Z. C. Mu, F. Li, S. M. Jiang, J. Y. Zhang, H. X. Zhang, Y. Wang and C. M. Che, *J. Phys.Chem. B,* 2005, **109**, 8008.
17 D. J. Abdallah, R. G. Weiss, *Langmuir*, 2000, **16**, 352.
18 M. Han and K. Ichimura, *Macromolecules*, 2001, **34**, 82.
19 (a) R. G. Snyder, H. L. Strauss, C. A. Elliger, *J. Phys. Chem.*, 1982, **86**, 5145; (b) R. A. MacPhail, H. L. Strauss, R. G. Snyder, C. A. Elliger, *J. Phys. Chem.*, 1984, **88**, 334; (c) N. V. Venkataraman, S. Vasudevan, *J. Phys. Chem. B*, 2001, **105**, 1805.
20 C. Xue, S. Jin, X. Weng, J. J. Ge, Z. Shen, H. Shen, M. J. Graham, J. K. Jeong, H. Huang, D. Zhang, M. Guo, F. W. Harris, S. Z. D. Cheng, *Chem. Mater.*, 2004, **16**, 1014.
21 (a) M. Shimomura and T. Kunitake, *J. Am. Chem. Soc.*, 1987, **109**, 5175; (b) H. Kobayashi, K. Koumoto, J. H. Jung and S. Shinkai, *J. Chem. Soc., Perkin Trans.*, 2002, **2**,1930.